COMPUTATIONAL PROBLEMS OF ELECTRICAL ENGINEERING

Vol. 12, No. 1, 2022

SCATTERING OF PLANE WAVES BY AN OPEN ARC WITH DIFFERENT BOUNDARY CONDITIONS ON ITS SIDES

Volodymyr Emets
Lodz University of Technology, Poland
volodymyr.yemyets@p.lodz.pl
https://doi.org/10.23939/jcpee2022.01.017

Abstract: The paper considers an approach to numerical modelling of the problem of electromagnetic plane waves scattering by an open arc with different boundary conditions on its sides. The corresponding mixed boundary value problem is reduced to a system of two singular and hypersingular integral equations. The method of collocation for numerical solutions to the equations obtained is proposed and analyzed. Numerical results of the radar cross-section for different values of arc curvatures are presented.

Key words: electromagnetic waves scattering; numerical modeling; collocation method; mixed boundary conditions.

1. Introduction

The problem of scattering field determination by a strip with different boundary conditions on its sides has attracted attention in the past decades [1–5]. In this paper, we consider the direct scattering problem for an open arc with mixed boundary conditions. This kind of problem is of fundamental importance in the modelling of many practical problems like antennas design, nondestructive control of the buried objects, etc. The solution to the Dirichlet, Neumann and impedance problems has only a square root singularity at the arc tips. This singularity can be eliminated from consideration using the cosine substitution [6–11] or with the introduction of the additional condition [12]. The purpose of this paper is to give an efficient computing method for the determination of the scattered waves for the open arc with different boundary conditions on its sides, using the collocation method without considering the different structure of the solution singularities at tips.

2. Arc with mixed boundary condition

The problem being considered here is shown in Fig. 1 on the x_1, x_3 – plane. The arc occupies a domain $\Gamma = \left\{\mathbf{x}(s) : \mathbf{x}(s) \in C^2, s \in [b,a]\right\} \subset R^2$, where $x = (x_1; x_3)$ are the Cartesian coordinates and $J(s) = |\mathbf{x}'(s)| \neq 0$ is the Jacobean. The orientation of Γ is assumed to be from the end point $x(b)$ to the end point $x(a)$. Further, we denote by Γ_+ and Γ_- the upper and lower sides of Γ, respectively, **n** is the unit external normal vector to Γ_+.

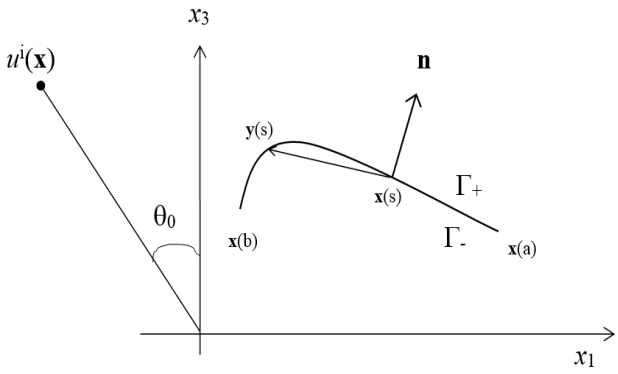

Fig. 1. Geometry of the problem

A plane wave

$$u^i(\mathbf{x}) = e^{ik(\mathbf{l},\mathbf{x})}, \mathbf{l} = (\sin\theta_0, -\cos\theta_0), \qquad (1)$$

impinges on the arc. The time factor $e^{-i\omega t}$ is omitted in the analysis. Here $(.,.)$ is the scalar product, k is the wave number, and θ_0 is the incident angle.

The total field $u = u^s + u^i$ consists of the given incident wave u^i and the unknown scattered wave u^s. The scattered wave satisfies the Sommerfeld radiation condition at infinity that implies:

$$u(\mathbf{x}) = \frac{e^{ik|\mathbf{x}|+i\pi/4}}{\sqrt{8\pi k|\mathbf{x}|}} f(k,\mathbf{l},\mathbf{v}), |\mathbf{x}| = \sqrt{x_1^2 + x_3^2} \to \infty . \quad (2)$$

Here $f(k,\mathbf{l},\mathbf{v})$ is the complex amplitude or far-field pattern of the scattering wave and $\mathbf{v} = (\sin\theta, \cos\theta)$ is the direction of observation.

The mathematical modelling for the time-harmonic electromagnetic waves scattering from thin infinitely long cylindrical coated object leads to the following mixed boundary value problem for the Helmholtz equation in the exterior domain of the inhomogeneity:

$$\left(\Delta + k^2\right)u = 0, \tag{3}$$

with the following conditions along the boundary $\Gamma_0 = \Gamma / \left\{x(b), x(a)\right\}$

$$\frac{\partial u_+(\mathbf{x})}{\partial n_x} = 0,\ u_-(\mathbf{x}) = 0, \tag{4}$$

were

$$u_-(\mathbf{x}) = \lim_{\varepsilon\to 0} u(\mathbf{x} - \varepsilon\mathbf{n}),$$

$$\frac{\partial u_+(\mathbf{x})}{\partial n_x} = \lim_{\varepsilon\to 0}\left(\mathbf{n}_x, \nabla u(\mathbf{x} + \varepsilon\mathbf{n})\right),\ \mathbf{n}_x = \frac{(x_3', -x_1')}{J(s)}$$

exists for all $\mathbf{x}\in\Gamma_0$ locally uniformly.

Boundary conditions (4) admit several interpretations. For the electric field with E_2-component, the upper side is a perfect magnetic conductor (PMC) and the lower side is a perfect electric conductor (PEC). On the other hand, for the magnetic field with H_2-component, the upper side is PEC while the lower side is PMC.

By using Green's theorem, the integral representation of the scattering field can be represented as

$$u^s(\mathbf{x}) = k\int_\Gamma\left[k^{-1}\Phi_3(\mathbf{y})\frac{\partial g(\mathbf{x},\mathbf{y})}{\partial n_y} - \Phi_1(\mathbf{y})g(\mathbf{x},\mathbf{y})\right]d\Gamma_y$$

$$k\Phi_1(\mathbf{y}) = \left(\frac{\partial u_+(\mathbf{y})}{\partial n_y} - \frac{\partial u_-(\mathbf{y})}{\partial n_y}\right), \tag{5}$$

$$\Phi_3(\mathbf{y}) = u_+(\mathbf{y}) - u_-(\mathbf{y}),$$

$$g(\mathbf{x},\mathbf{y}) = \frac{i}{4}H_0^{(1)}\left(k|\mathbf{x}-\mathbf{y}|\right),\ \mathbf{y} = (y_1.y_3).$$

Herein $H_n^{(1)}$ is the Hankel function of the first kind of order n and $g(x; y)$ is the fundamental solution to equation (3).

For scattering amplitude (2) from (5) we have

$$f(k,\mathbf{l},\mathbf{v}) = -k\int_\Gamma\left[\Phi_1(\mathbf{y}) + i(\mathbf{v},\mathbf{n}_y)\Phi_3(\mathbf{y})\right]e^{-ik(\mathbf{v},\mathbf{y})}d\Gamma_y. \tag{6}$$

The following system of integral equations for $\Phi_\beta(x_1),\ \beta = 1, 3$ are obtained from Eqs. (1), (2) and (5)

$$\Phi_1(\mathbf{x}) + i\frac{k}{2}\int_\Gamma\Phi_3(\mathbf{y})G_1(\mathbf{x},\mathbf{y})d\Gamma_y = -2i(\mathbf{l},\mathbf{n}_x)e^{ik(\mathbf{l},\mathbf{x})}, \tag{7}$$

$$\Phi_3(\mathbf{x}) + i\frac{k}{2}\int_\Gamma\Phi_1(\mathbf{y})G_3(\mathbf{x},\mathbf{y})d\Gamma_y = 2e^{ik(\mathbf{l},\mathbf{x})},\ \mathbf{x}\in\Gamma_0$$

$$G_1(\mathbf{x},\mathbf{y}) = H_2^{(1)}\left(k|\mathbf{x}-\mathbf{y}|\right)\frac{\partial|\mathbf{x}-\mathbf{y}|}{\partial\mathbf{n}_x}\frac{\partial|\mathbf{x}-\mathbf{y}|}{\partial\mathbf{n}_y} +$$

$$+\frac{H_1^{(1)}\left(k|\mathbf{x}-\mathbf{y}|\right)}{k|\mathbf{x}-\mathbf{y}|}\left(\mathbf{n}_x,\mathbf{n}_y\right),\ G_3(\mathbf{x},\mathbf{y}) = H_0^{(1)}\left(k|\mathbf{x}-\mathbf{y}|\right).$$

Considering that

$$H_0^{(1)}(z) = a_0 + \frac{2i}{\pi}\ln z,\ \frac{H_1^{(1)}(z)}{z} = b_0 - \frac{2i}{\pi z^2} + \frac{i}{\pi}\ln z,$$

$$H_2^{(1)}(z) = -\frac{4i}{\pi z^2} - \frac{i}{\pi},\ \left(\mathbf{n}_x,\mathbf{n}_y\right) = 1,$$

when $z = |\mathbf{x}-\mathbf{y}| \to 0$, from (7) we get

$$G_1(\mathbf{x},\mathbf{y}) = -\frac{2i}{\pi\left(k|\mathbf{x}-\mathbf{y}|\right)^2} + \frac{i}{\pi}\ln\left(k|\mathbf{x}-\mathbf{y}|\right) + b_1(\mathbf{x}) + K_1(\mathbf{x},\mathbf{y}),$$

$$G_3(\mathbf{x},\mathbf{y}) = a_0 + \frac{2i}{\pi}\ln\left(k|\mathbf{x}-\mathbf{y}|\right) + K_3(\mathbf{x},\mathbf{y}),$$

$$a_0 = 1 + \frac{2i}{\pi}(\gamma - \ln 2),\ b_0 = \frac{1}{2} + \frac{i}{\pi}\left(-\frac{1}{2} + \gamma - \ln 2\right),$$

$$b_1 = b_0 - \frac{i}{\pi k^2}K^2,\ K = \frac{x_1'x_3'' - x_3'x_1''}{J^3},$$

where γ is the Euler constant, K is the curvature of the curve Γ_0 at the point s, $K_\beta(\mathbf{x},\mathbf{y}),\ \beta = 1, 3$ are the regular functions: $K_\beta(\mathbf{x},\mathbf{x}) = 0$. Thus, the kernels of integral equations (7) can be split into singular and regular parts. The integral with the unknown function $\Phi_3(\mathbf{y})$ must be understood in the Hadamard sense and the integral with $\Phi_1(\mathbf{y})$ has a logarithm singularity.

3. Method of collocation

All integrals with the regular functions can be computed by the standard trapezoidal quadrature, however for hypersingular and weakly singular integrals the improved integration procedure must be applied. Consider the following hypersingular integral

$$I(s_m) = \int_b^a \Psi(\tau)\frac{d\tau}{|s_m - \tau|^2},$$

where $\Psi(\tau)$ is a Hőlder function on $[b,a]$, and the set of N nodes are used:

$$\tau_m = b + (m-1)h,\ m = 1,\ldots,N+1,$$

$$s_n = b + (n - 1/2)h,\ n = 1,\ldots,N+1,\ h = \frac{a-b}{N}.$$

The integral $I(s_m)$ can be replaced by the quadrature sum:

$$I(s_m)=\sum_{n=1}^{N}\Psi(s_n)S_{nm},\ S_{nm}=\frac{1}{s_m-\tau_{n+1}}-\frac{1}{s_m-\tau_n},\quad (8)$$

that converges uniformly to the value of $I(s_m)$ when $N\to\infty$ and for the discrete approximation of the logarithmic integral, we get [4]:

$$\begin{aligned}&\int_b^a\Phi(\tau)\ln\left[x\left|\mathbf{x}(s_n)-\mathbf{y}(\tau)\right|\right]d\tau=\\&=\int_b^a\Phi(\tau)\ln x\frac{\left|\mathbf{x}(s_n)-\mathbf{y}(\tau)\right|}{\left|s_n-\tau\right|}d\tau+\\&+\int_b^a\Phi(\tau)\ln\left|s_n-\tau\right|d\tau=\\&=\sum_{m=1}^{N}\Phi(s_m)\left[h\ln x\frac{\left|\mathbf{x}(s_n)-\mathbf{x}(s_m)\right|}{\left|s_n-s_m\right|}+L_{nm}\right],\\&L_{nm}=(\tau_{m+1}-s_m)\left(\ln\left|\tau_{m+1}-s_m\right|-1\right)-\\&-(\tau_m-s_m)\left(\ln\left|\tau_m-s_n\right|-1\right)\end{aligned}\quad (9)$$

Thus, using quadrature formulae (8) and (9), from (7) we have the following system of algebraic equations:

$$\begin{aligned}&\Phi_{1m}+\frac{i}{2}k\sum_{n=1}^{N}\Phi_{3n}A_{nm}J(s_n)=\\&=-\frac{2i}{J(s_m)}\left(l_1x'_{3m}-l_3x'_{1m}\right)e^{ik(\mathbf{l},\mathbf{x}_m)},\\&\Phi_{3n}+\frac{i}{2}k\sum_{m=1}^{N}\Phi_{1m}B_{nm}J(s_m)=2e^{ik(\mathbf{l},\mathbf{x}_n)},\\&A_{nm}=-\frac{2i}{\pi k^2}\frac{(s_m-s_n)^2}{\left|\mathbf{x}(s_n)-\mathbf{x}(s_m)\right|^2}S_{nm}+\\&+\frac{i}{\pi}\left(h\ln k\frac{\left|\mathbf{x}_n-\mathbf{x}_m\right|}{\left|s_n-s_m\right|}+L_{mn}\right)+h(b_1+K_{3nm}),\\&B_{mn}=\frac{2i}{\pi}\left(h\ln\left(k\frac{\left|\mathbf{x}_n-\mathbf{x}_m\right|}{\left|s_n-s_m\right|}\right)+L_{nm}\right)+h(a_0+K_{3nm}),\\&\Phi_{1m}=\Phi_1(\mathbf{x}_m),\ \Phi_{3n}=\Phi_3(\mathbf{x}_n),\\&K_{\beta nm}=K_\beta(\mathbf{x}_n,\mathbf{x}_m),\ \mathbf{x}_n=\mathbf{x}(s_n),\\&n,m=1,2,...,N.\end{aligned}\quad (10)$$

Here

$$\frac{\left|\mathbf{x}(s)-\mathbf{x}(\tau)\right|}{\left|s-\tau\right|}=J(s),$$

when $\tau=s$ and it means that singularities of equations (7) have been removed.

The difference between the solutions to linear algebraic system (10) and the solutions of integral equations (7) tends to zero when the truncation parameter N tends to infinity. Finally, the scattering amplitude relates to the coefficients Φ_{1m} and Φ_{3n} as follows:

$$\begin{aligned}&f(k,\mathbf{l},\mathbf{v})=-kh\sum_{m=1}^{N}\Phi_{1m}e^{-ik(\mathbf{v},\mathbf{x}_m)}J(s_m)-\\&-ikh\sum_{n=1}^{N}\Phi_{3n}\left[v_1x'_3(s_n)-v_3x'_1(s_n)\right]e^{-ik(\mathbf{v},\mathbf{x}_n)}.\end{aligned}$$

4. Numerical examples

In this section, we will demonstrate our numerical method through some examples. The numerical results of the backscattering cross-section

$$\sigma(\theta_0)=20\log_{10}\frac{\left|f(k,\mathbf{l},-\mathbf{l})\right|}{4x}$$

for $x=kd_0=3\pi$ are presented in Figs. 2–4 and accuracy of one percent is obtained when the truncation parameters $N, M = 4x$. In the first example, Γ_0 is an ellipse arc:

$$\Gamma_0=d_0(\cos s,\varepsilon\sin s),\ s\in[0,\pi],\ d_0,\ \varepsilon=const.$$

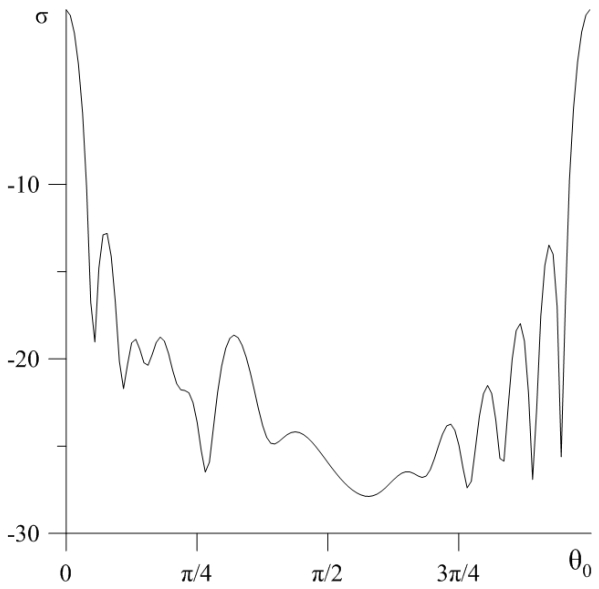

Fig. 2. $\sigma(\theta_0)$ *versus* θ_0 *for a strip*

In Fig. 2 the scattered characteristic $\sigma(\theta_0)$ for a strip $(\varepsilon=0)$ is shown. It should be noted that the obtained curve is in a good coincidence with the previously obtained one by using the method of

moments [2] and with the curve obtained on the base of high frequency asymptotic [4]. Analogously, the results for the two different arcs with $\varepsilon = 1$ and $\varepsilon = -1/4$ are shown in Fig. 3. As it can be observed, the tips of the arc and the boundary conditions on its sides are not much affected on the backscattering field if they are in the shadow domain. This feature can be observed also in the second example, shown in Fig. 4, where $\Gamma_0 = d_0(s, \sinh s)$, $s \in [-1, 1]$. As could be expected, the backscattering far-field take the maximum values when the backscattering directions are close to the directions of the external normal vector to the arc.

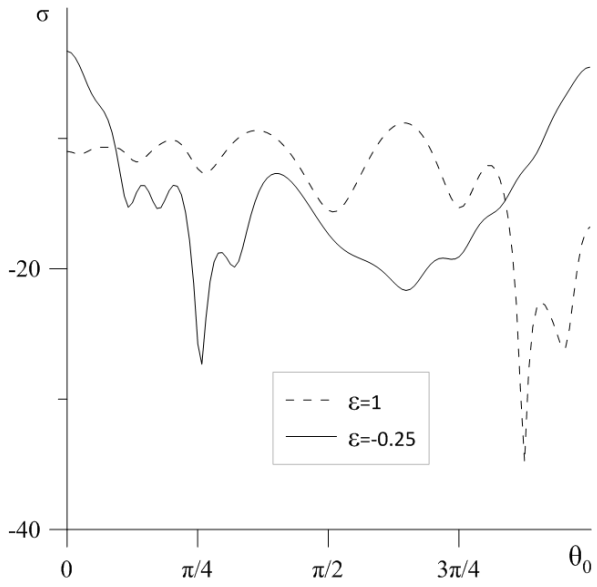

Fig. 3. $\sigma(\theta_0)$ *versus* θ_0 *for an arc* $(\cos s, \varepsilon \sin s)$, $s \in [0, \pi]$ *with* $\varepsilon = 1$ *and* $\varepsilon = -0.25$.

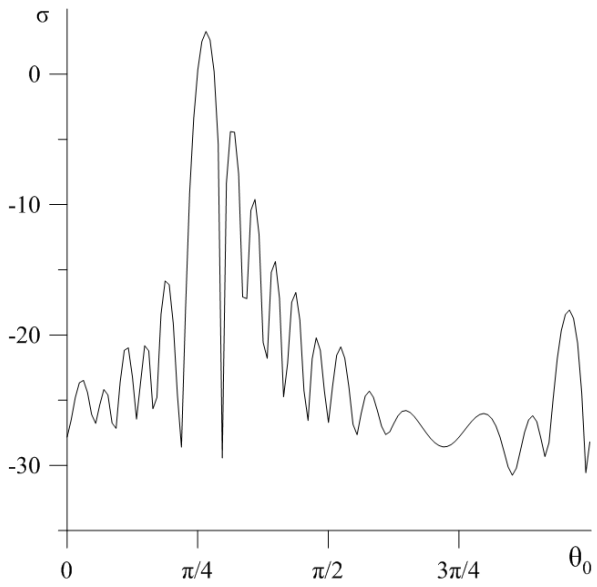

Fig. 4. $\sigma(\theta_0)$ *versus* θ_0 *for an arc* $(s, \sinh s)$, $s \in [-1, 1]$

5. Conclusion

The numerical solution in modelling of the scattering problem from an open arc with the mixed boundary condition on its sides is constructed. The problem is reduced to a system of the hyper and weak singular integral equations. In order to solve the obtained integral equations, the collocation method is developed. The numerical examples are presented for the radar cross-sections as the functions of the incidence angles and the different curvature values of arcs.

Acknowledgment

Calculation results of this paper were obtained in collaboration with Dr Jan Rogowski.

5. References

[1] G. Apaydin, F. Hacivelioglu, L. Sevgi, and P. Ufimtsev, "Fringe waves from a wedge with one face electric and the other face magnetic", *IEEE Transactions on Antennas and Propagation*, vol. 64, pp. 1125–1130, Mar. 2016.

[2] G. Apaydin and L. Sevgi, "Method of moments modeling of backscattering by a soft-hard strip", *IEEE Transactions on Antennas and Propagation*, vol. 63, pp. 5822–5826, 2015.

[3] F. Hacivelioglu, L. Sevgi, and P. Y. Ufimtsev, "Method of moments modeling of backscattering by a soft-hard strip", *Backscattering from a soft-hard strip: Primary edge waves approximations*, vol. 12, pp. 249–252, 2013.

[4] V. Emets and J. Rogowski, "Scattering from a strip with mixed boundary conditions", *Radio Science*, vol. 55, no. 11, pp. 1–8, 2020.

[5] M. A. Uslu, G. Apaydin, and L. Sevgi, "Diffraction modeling by a soft/hard strip using finite-difference time-domain method", *IEEE Antennas Wireless Propag. Lett.*, vol. 16, pp. 306–309, 2017.

[6] R. Kress, "Inverse scattering from an open arc", *Math. Method. Appl. Sci.*, vol. 18, no. 4, pp. 267–293, 1995.

[7] R. Kress and K. M. Lee, "Integral equation methods for scattering from an impedance crack", *J. Comp. Appl. Math.*, vol. 61, pp. 161–177, 2003.

[8] K. M. Lee, "Inverse scattering problem for an impedance crack", *Wave Motion*, vol. 45, pp. 254–263, 2008.

[9] H. Li, J. Huang, and G. Zeng, "On the numerical solutions of two-dimensional scattering problems for an open arc", *Boundary Value Problems*, vol. 136, pp. 1–15, 2020.

[10] L. Monch, "On the numerical solution of the direct scattering problem for a sound-hard open arc", *Comput. Appl. Math.*, vol. 71, pp. 343–356, 1996.

[11] "On the inverse acoustic scattering problem by an open arc: the sound-hard case", *Inverse Probl*., vol. 13, pp. 1379–1392, 1997.

[12] J. J. Liu, P. A. Krutitskii, and M. Sini, "Numerical solution of the scattering problem for acoustic waves by a two-side crack in 2-d dimensional space", *Journal of Computational Mathematics*, vol. 29, no. 2, pp. 141–166, 2011.

РОЗСІЯННЯ ПЛОСКИХ ХВИЛЬ ВІДКРИТОЮ ДУГОЮ ІЗ РІЗНИМИ ГРАНИЧНИМИ УМОВАМИ НА ЇЇ СТОРОНАХ

Володимир Ємець

У роботі розглянуто підхід до чисельного моделювання проблеми розсіяння електромагнітних плоских хвиль на незамкненій дузі із різними граничними умовами на її сторонах. Відповідна змішана крайова задача зводиться до системи двох сингулярних і гіперсингулярних інтегральних рівнянь. Запропоновано та проаналізовано метод колокації для отримання числових розв'язків одержаних рівнянь. Наведено характеристики поперечного перерізу розсіяння для різних значень кривизни дуги.

Volodymyr Emets, born 28.04.1956 in Khmelnytsky, Ukraine. Graduated from the Mechanical – Mathematical Department of Lviv State University in 1978, received PhD, DSc degrees and a title professor in 1985, 1997 and 2003, respectively.

He has been working as a professor at the Institute of Computer Science of Lodz University of Technology, Poland since 2000.

His research is concerned with mathematical problems of electromagnetic and elastics waves diffraction, including analytical- numerical methods of the singular and hypersingular integral equations solutions.

Received: 04.01.2022. Accepted: 25.03.2022